JPET Fast Forward. Published on March 9, 2017 as DOI: 10.1124/jpet.116.239137
This article has not been copyedited and formatted. The final version may differ from this version.

Mogroside IIIE, a novel anti-fibrotic compound, reduces pulmonary fibrosis through Toll like receptor 4 pathways

Lijun Tao, Jinyu Yang, Fengyan Cao, Haifeng Xie, Mian Zhang, Yanqing Gong and Chaofeng Zhang

Research Department of Pharmacognosy, China Pharmaceutical University, Nanjing, 211198, People's Republic of China;

Division of Translational Medicine and Human Genetics, Department of Medicine, Perelman School of Medicine, University of Pennsylvania, Philadelphia, PA, 19104, United State;

Chengdu biopurity phytochemicals Ltd. Chengdu, 611131, People's Republic of China

JPET Fast Forward. Published on March 9, 2017 as DOI: 10.1124/jpet.116.239137
This article has not been copyedited and formatted. The final version may differ from this version.

Running title: MGIIIE prevents bleomycin-induced pulmonary fibrosis

Corresponding author:

Yanqing Gong

Assistant Professor

Division of Translational Medicine and Human Genetics; Department of Medicine, Perelman School of Medicine. University of Pennsylvania. Smilow Center for Translational Research, Room 11-142, Philadelphia, PA, 19104, United States

Phone: 215 746 3510 Fax: 215 573 8606 E-mail: gongy@mail.med.upenn.edu

Chaofeng Zhang (C.F. Zhang)

Associate professor

Research Department of Pharmacognosy. China Pharmaceutical University. 639 Longmian Road, Nanjing 210098 PR China

Phone/Tax: +(86)25 8618 5140 E-mail: zhangchaofeng@cpu.edu.cn

Text pages 35

Figures 7

Tables 1

References 48

Words in the abstract 224

Words in the introduction 539

Words in the discussion 988

Nonstandard abbreviations

α-SMA, α-smooth muscle actin; BIBF 1120, nintedanib; BSA, bovine serum albumin; cDNA, complementary DNA; Col I, type I collagen; DAB, diaminobenzidine;

JPET Fast Forward. Published on March 9, 2017 as DOI: 10.1124/jpet.116.239137
This article has not been copyedited and formatted. The final version may differ from this version.

DMEM, Dulbecco's Modification of Eagle's Medium; ECL, enhanced chemiluminescence; ECM, extracellular matrix; ERK, extracellular signal-regulated kinase; FBS, fetal bovine serum; H&E, Hematoxylin-eosin; IPF, idiopathic pulmonary fibrosis; JNK, c-JUN N-terminal kinase; LPS, lipopolysaccharide; MAPKs, mitogen activated protein kinases; MGIIIE, mogroside IIIE; MGIVE, mogroside IVE; MGV, mogroside V; PLFs, primary mouse lung fibroblasts; MMP-9, metalloproteinases-9; MPO, myeloperoxidase; MyD88, myeloid differentiation factor 88; PBS, phosphate-buffered saline; PMSF, phenylmethanesulfonyl fluoride; SDS-PAGE, sodium dodecyl sulfate polyacrylamide gel electrophoresis; Smads, Sma-and Mad-related proteins; SMI, siamenoside I; TGF-β, transforming growth factor-β; TIMP-1, tissue inhibitor of metalloproteinase-1; TLR4, toll-like receptor 4.

Section

Gastrointestinal, Hepatic, Pulmonary, and Renal

Abstract

Idiopathic pulmonary fibrosis (IPF) is a progressive fibrotic lung disease and eventually, most of patients were subjected to respiratory failure with a median survival of 2 to 3 years after diagnosis due to a lack of effective therapies in clinic. Mogroside IIIE (MGIIIE), a cucurbitane-type compound, was isolated from *Siraitia grosvenorii*. MGIIIE has shown strongest inhibition of NO release, a crucial inflammatory factor, from LPS-treated RAW264.7 cells compared with other mogrosides. In pulmonary fibrosis mouse model induced by bleomycin, MGIIIE treatment attenuated pulmonary fibrosis indicated as a reduction in myeloperoxidase (MPO) activity, collagen deposition as well as pathological score. Second, MGIIIE significantly suppressed expression of several important fibrotic markers e.g. α-SMA, collagen I, TGF-β signal and MMP-9/TIMP-1. Furthermore, MGIIIE blocked tansdifferentiation of lung resident fibroblasts into myofibroblast-like cells induced by TGF-β or LPS and subsequently inhibited collagen production in lung fibroblasts. These data indicate that MGIIIE is a potent inhibitor for pulmonary fibrosis. *In vitro* and *in vivo* mechanistic studies have shown that MGIIIE significantly decreased expression of TLR4 and its downstream signals MyD88-MAPK, an inflammatory signal essential for extracellular matrix (ECM) deposition in pulmonary fibroblasts. Taken together, these results demonstrate that MGIIIE significantly prevents pulmonary fibrosis by inhibiting pulmonary inflammation and ECM deposition through regulating TLR4/MyD88-MAPK signaling. Our study suggests that MGIIIE may have therapeutic potential for treating pulmonary fibrosis in clinic settings.

JPET Fast Forward. Published on March 9, 2017 as DOI: 10.1124/jpet.116.239137
This article has not been copyedited and formatted. The final version may differ from this version.

1. Introduction

Idiopathic pulmonary fibrosis (IPF) is a severe lung disease and characterized by progressive and irreversible destruction of lung architecture caused by excessive extracellular matrix (ECM) deposition that ultimately leads to respiratory failure. The median survival time of patients with IPF is about 2 or 3 years due to limited clinic therapies (Gürbüzel et al., 2016). Extensive evidences indicate that dysfunctions of resident fibroblasts by lung inflammation greatly contribute to the development of pulmonary fibrosis. Once fibroblasts become activated, they transform into α-smooth muscle actin-expressing myofibroblasts that secrete ECM components leading to fibrotic lesion in lung (Derynck and Zhang, 2003; Chen et al., 2012). A variety of cytokines and proteinases have shown involved in fibrotic process including TGF-β, MPO, MMPs (Bhattacharyya et al., 2013; Shi et al., 2014; Yoshimura et al., 2006), which are considered as essential makers for pulmonary fibrosis. Recently, a crucial role of toll like receptor 4 (TLR4) in fibroblasts during fibrogenesis has been highlighted (Poltorak et al., 1998; Jiang et al., 2005; Huebener and Schwabe, 2013). Pulmonary fibrosis induced by bleomycin, lipopolysaccharide (LPS) or radiation was significantly attenuated in TLR4 knock out mice (Bhattacharyya et al., 2013; He et al., 2009; He et al., 2012; Rhieu et al., 2014). Moreover, it has been reported that TLR4 is required for fibroblast activation and collagen production as indicated that transforming growth factor-β (TGF-β) failed to induce collagen production in TLR4 knockout fibroblasts (Bhattacharyya et al., 2013). Up-regulated TLR4 in fibroblasts augmented TGF-β sensitivity and converted self-limited tissue repair into intractable fibrosis in bleomycin-induced pulmonary fibrosis (Bhattacharyya et al., 2013). In addition, downstream signals of TLR-4, MAPKs, including ERK, JNK, and p38, were significantly activated in lung tissue from IPF patients (Yoshida et al., 2002) and

blockade of ERK, JNK and p38 reduced fibrosis in mouse models (Vittal et al., 2013; Matsuoka et al., 2002; Madala et al., 2012; van der Velden et al., 2016). Therefore, disruption for TLR4 over-expression in lung inflammation may represent a potential target for IPF prevention.

The fruits of *Siraitia grosvenorii* (Cucurbitaceae), a famous traditional Chinese medicine, is utilized for the treatments of dry cough, sore throat, extreme thirst and constipation (Committee of National Pharmacopoeia, 2010; Chen et al., 2011) in China. The active components of Cucurbitaceae are a group of cucurbitane-type triterpene glycosides named as mogrosides. It is reported that mogrosides has various bioactivities, including anti-inflammatory, anti-obesity, anti-diabetic and anti-allergic effects as well as hepatoprotective effects (Chen et al., 2011; Di et al., 2011; Sun et al., 2012; Jin and Lee, 2012; Xiao et al., 2012; Xiao and Wang, 2013; Song et al., 2014). Recent research has shown Mogroside V attenuated LPS-induced acute lung injury and inflammation (Shi et al., 2014; Xu et al., 2015; Suzuki et al., 2005), however, anti-fibrotic effects of mogrosides on respiratory diseases have not been reported.

Mogroside IIIE (MGIIIE) is a main component of fruits of *Siraitia grosvenorii* and has shown strongest anti-inflammatory effects in LPS-induced macrophage activation in our screening experiment. Therefore, MGIIIE was selected for evaluating anti-fibrotic effects in a mouse experimental model of pulmonary fibrosis. MGIIIE exhibited a significant anti-fibrotic activity in both *in vitro* and *in vivo* models. Mechanistic studies identified that the MGIIIE inhibition fibrosis may be dependent on TLR4 mediated MAPKs signaling pathways.

2. Materials and methods

2.1. Chemicals and reagents

Mogroside IIIE (MGIIIE, purity above 99%), Mogroside IVE (MGIVE, purity

JPET Fast Forward. Published on March 9, 2017 as DOI: 10.1124/jpet.116.239137
This article has not been copyedited and formatted. The final version may differ from this version.

above 99%), Siamenoside I (SMI, purity above 99%) and Mogroside V (MGV, purity above 99%) were all purchased from Chengdu Biopurify Phytochemical Ltd. (Chengdu, China). The purity of these Mogrosides has been tested by HPLC. Bleomycin was obtained from Nippon Kayaku (Tokyo, Japan). Prednisone was obtained from Zhejiang Xianju Pharmaceutical Co., Ltd. (Xianju, China). Recombinant TGF-β_1 was purchased from PeproTech Inc. (Rocky Hill, NJ). TAK-242 (a TLR4 inhibitor) was purchased from Merck Millipore Inc. (Billerica, USA). 3-(4, 5-dimethylthiazol-2-yl)-2,5-diphenyl tetrazolium bromide (MTT) was obtained from Biosharp Technology Inc. (Hefei, China).

Myeloperoxidase (MPO) test kit was purchased from Nanjing Jiancheng Bioengineering Institute (Nanjing, China). Antibodies against phospho-Smad2/3, p38/phospho-p38, ERK/phospho-ERK and JNK/phospho-JNK were all obtained from Cell Signal Technology Inc. (Massachusetts, USA). Antibodies against β-actin, α-SMA, MMP-9, TIMP-1, MyD88, TGF-β1, Smad2/3 and HRP-conjugated secondary antibody were all purchased from Bioworld Technology Inc. (Dublin, OH, USA). Antibody against Col I was purchased from Wanleibio Technology Inc. (Shenyang, China). Antibody against TLR4 and secondary antibody Donkey anti-rabbit IgG H&L (Alexa Fluor 488) were obtained from Abcam Technology Inc. (Cambridge, UK). DAPI was obtained from Nanjing KeyGEN Biotech. Co., Ltd. (Nanjing, China).

2.2. Animals

Adult male C57BL/6 mice weighing between 20±2 g (6–8 weeks old) were purchased from Comparative Medicine Center of Yangzhou University (Yangzhou, China). Animals were taken care according to General Recommendation and Provisions of the Chinese Experimental Animals Administration Legislation. The

animal protocol was approved by the Institutional Ethical Committee of China Pharmaceutical University. Mice were housed in a climate-controlled room at 22±2°C and 50±10% humidity with a 12 h light/dark cycle, and given conventional feed, free drinking water.

2.3. RAW 264.7 culture and Nitric oxide (NO) measurement

RAW 264.7 cell line was purchased from the Cell Bank of Chinese Academic of Sciences (Shanghai, China). RAW264.7 cells were maintained in Dulbecco's Modification of Eagle's Medium (DMEM, GIBCO, NY, USA) supplemented with 10% FBS (Hyclone, Thermo, South America), penicillin (100 U/ml) and streptomycin (100 μg/ml) at 37°C, with 95% humidity and 5% carbon dioxide. For treatment, RAW264.7 cells were detached and seeded in 96-well plates at 4×10^4 cells per well. When reaching a confluence of 70%-80%, cell were incubated with LPS (5 μg/ml), chemicals or controls (PBS or DMSO) for 24 h. 50 μl cell medium was used for NO measurement according to a previous publication (Fan et al., 2013). Briefly, 50 μl of the Griess reagent (Beyotime, China) was mixed with 50 μl culture medium. After standing for 5 min, the optical density of mixture was measured by a microplate reader at 540 nm wavelength. The concentration of nitrite was determined by a standard curve using sodium nitrite.

2.4. Experimental model of bleomycin-induced pulmonary fibrosis in mice

The method of bleomycin-induced pulmonary fibrosis was described as previously (You et al., 2015). Briefly, after one week of acclimation, animals were divided randomly into six groups and anesthetized by intraperitoneal injection of chloral hydrate solution (4%, 10 ml/kg), then followed by intratracheal instillation respectively of bleomycin (5 mg/kg) or saline as control. Seven days later after bleomycin administration, MGIIIE-H (20 mg/kg), MGIIIE-M (10 mg/kg) and

JPET Fast Forward. Published on March 9, 2017 as DOI: 10.1124/jpet.116.239137
This article has not been copyedited and formatted. The final version may differ from this version.

MGIIIE-L (1 mg/kg) were orally administered to mice once a day for 14 consecutive days. Prednisone (6.5 mg/kg) was used as positive drug. The control groups were given the same volume of 0.9% sterilized saline. On the day of 21, mice were euthanized by excessive intraperitoneal injection of chloral hydrate. Lung tissue was excised for pulmonary index measurement (lung weight/body weight; mg/g). The left lower lobes were fixed in 10% formalin for histopathological examination, and the rest of lung tissue was stored at -80°C.

2.5. Histological analysis

The lung tissue was fixed with 10% formalin were embedded in paraffin, sectioned, and stained with Hematoxylin-eosin (H&E) or Masson's trichrome. Pathological evaluation was conducted by experienced pathologists in a single-blind way. The results were scored in accordance with the previously reported method (Szapiel et al., 1979), and the score numbers (0–3) were respectively corresponded to the grades of -, +, ++ and +++.

2.6. MPO and IL-1β assays

Myeloperoxidase (MPO) was an indicator of polymorphonuclear leukocyte accumulation. The method of MPO assay was described previously (Shi et al., 2014). Briefly, 21 days after bleomycin treatment, right lungs were excised, homogenized in extraction buffer. After centrifuging, the homogenate and reaction buffer were mixed and heated to 37°C for 15 min. The enzymatic activity was measured by a 96-well plate reader at 460 nm wavelength.

IL-1β levels in the lung tissue homogenate were measured with ELISA kit according to the instructions recommended by the manufactures. The optical density of the microplate was read at 450 nm by a 96-well plate reader.

2.7. Isolation and culture of primary mouse lung fibroblasts

JPET Fast Forward. Published on March 9, 2017 as DOI: 10.1124/jpet.116.239137
This article has not been copyedited and formatted. The final version may differ from this version.

The primary mouse lung fibroblasts (PLFs) were isolated as described previously, with some modifications (Bruce and Honaker, 1998). Briefly, Lung tissue collected from C57/BL6 mice were minced into 1- to 2-mm^3 pieces and digested with trypsin for 15 min at 37°C. The digested cell suspensions were collected and cultured with DMEM complete medium and incubated at 37°C in an atmosphere of 5% CO_2 in air over night. After cells attached, the medium was changed the next day. The percentage of fibroblast was identified as 95% by morphology under microscope.

2.8. Cell treatment

For TGF-β1-treated PLFs, cells were detached with 0.25% trypsinization and seeded in 96-well at 4×10^4 cells per well or 6-well plates at 2×10^5 cells per well. Cells were treated with TGF-β1 (10 ng/ml), MGIIIE (10 μM) or controls (PBS or DMSO) for 48 h. For LPS-treated PLFs, cells were treated with LPS (5 μg/ml), MGIIIE (10 μM) or controls (PBS or DMSO) for 48 h. In some experiment, cell were pretreated with or without TLR4 inhibitor, TAK-242 (10 nM) for 1.5 h and subsequently incubated with/without LPS (5 μg/ml), MGIIIE (10 μM) or controls (PBS or DMSO) for 48 h.

2.9. Cell viability assay

Cell viability was assayed by the MTT assay. Briefly, cells were seeded in 96-well plates at 4×10^4 cells per well and incubated in DMEM containing 10% FBS for 24 h. The cells were treated as described above, then 5 mg/ml MTT was added to the wells and incubated for additional 4 h at 37°C in an atmosphere of 5% CO_2 in air. After mix well, the optical density was measured at 490 nm.

2.10. Real time quantitative PCR analysis

Total RNA was extracted from the lung tissue using Trizol reagent (Invitrogen Life Technologies, USA), reverse-transcribed to complementary DNA (cDNA) using the

TransScript first-Strand cDNA Synthesis kit (TOYOBO, Japan) and stored at -80°C until reverse transcription. The relative gene expression was quantified by Q-PCR using SYBR® Premix Ex Taq™ (TaKaRa, China) in StepOne™ Real-Time PCR (Life technologies, USA). In each reaction, 0.5 μg of total RNA was reverse transcribed before the following PCR conditions: 94°C for 2 minutes followed by 40 cycles at 94°C for 15 seconds, 58°C for 30 seconds, 72°C for 30 seconds, with final extension at 72°C for 10 minutes. The sequences (5′ to 3′) for the primers were shown in Table 1 and data were quantified using the comparative Ct (ΔCt) method and presented as mean ratio to β-actin.

2.11. Immunohistochemistry and immunofluorescence stainings

For immunohistochemistry staining, the paraffin sections (5 μm) were incubated with 3% H_2O_2 to eliminate endogenous peroxidase. After antigen retrieval by heating, non-specific binding sites were blocked by 5% skim milk in PBS for 1 h, the sections were then incubated with primary antibody and second antibodies conjugated with HRP. Color was visualized by incubated section with diaminobenzidine (DAB). Images were acquired under an Olympus BX53 microscope.

For immunofluorescence staining, cell were fixed with 4% paraformaldehyde/PBS for 15 min, followed by incubation with 0.3% Triton X-100/PBS for 10 min, 2% BSA/PBS block solution for 2 h and probed with primary antibody overnight at 4°C. Alexa Fluor 488-conjugated secondary antibodies were used to amplify the signal. DAPI was used to stain nuclei. Images were obtained by fluorescent microscopy (Olympus IX53) or confocal laser scanning microscopy (Carl Zeiss).

2.12. Western blot analysis

Total proteins extracted from lung homogenate or cell lysate were lysed in ice-cold RIPA lysis buffer containing 1:100 dilution of phenylmethanesulfonyl fluoride (PMSF,

Beyotime, China). Protein concentrations were determined using BCA Protein Assay Kit (Beyotime, China). After boiling for 10 min, equal amounts of the protein (50 μg/lane) were separated by SDS-PAGE gel and transferred to PVDF membranes (Merck Millipore, Billerica, USA) that were probed with primary antibodies overnight at 4°C and HRP-labeled secondary antibodies at 25°C for 2 h and the bands were visualized using super ECL detection reagent (Beyotime, China).

2.13. Statistical analysis

All data were presented as means ± standard deviation (S.D.) from at least three independent experiments. One-way ANOVA and two-tailed Student's t-test were used to analyze differences among different groups (GraphPad Prism software version 5.0). Values of $p < 0.05$ were regarded statistically significant.

JPET Fast Forward. Published on March 9, 2017 as DOI: 10.1124/jpet.116.239137
This article has not been copyedited and formatted. The final version may differ from this version.

3. Results

3.1. Anti-inflammatory activity screening of Mogrosides on LPS-activated RAW264.7 cells

Mogroside V (MGV), Siamenoside I (SMI), Mogroside IVE (MGIVE) and Mogroside IIIE (MGIIIE) are major mogrosides from fruits of Cucurbitaceae (Fig. 1A). It is reported that Mogroside V has anti-inflammatory activity in lung inflammation (Shi et al., 2014). Using LPS-stimulated RAW264.7 mouse macrophages activation model, we screened the anti-inflammatory effects of these four mogrosides. No cell toxicity was observed in all four morgosides treated groups (Fig. 1B). After cells were treated with LPS (5 μg/ml) for 24 h, NO production was increased approximately 3 folds. All four mogrosides significantly inhibited NO production induced by LPS in a dose-dependent manner. MGIIIE has a lowest IC50 of 10.22 μM compared with other mogrosides (Fig. 1C), indicating a strongest anti-inflammatory effect of MGIIIE. Therefore, MGIIIE was selected for further *in vivo* studies.

3.2. MGIIIE protects against bleomycin-induced pulmonary fibrosis in mice

Bleomycin is commonly-used agent to induce an experimental IPF model in mice which is characterized by activated myofibroblasts that contribute to the exuberant fibrosis (Bhattacharyya et al., 2013). In this model, 7-9 days is the switch point from lung inflammation to fibrotic phase. In the present study, experimental pulmonary fibrosis was induced by a single intratracheal instillation of bleomycin (5 mg/kg). Three doses of MGIIIE, MGIIIE-L (1 mg/kg/day), MGIIIE-M (10 mg/kg/day) and MGIIIE-H (20 mg/kg/day) were orally administered for 14 days respectively, starting 7 days after bleomycin administration. As a positive control, prednisone, a

synthetic corticosteroid drug for IPF treatment in clinic was administrated into mice after bleomycin injection. After bleomycin treatment, MGIIIE-M and MGIIIE-H significantly protected mice from weight loss and death even better than prednisone treatment (Fig. 2A and B). Histologic changes in the lung, including edema, alveolar wall thickening and neutrophil infiltration in the lung parenchyma were observed in mice after bleomycin treatment. MGIIIE markedly inhibited these lung damages as shown in Fig 2C-F. Furthermore, we compared several inflammatory factors level in mice in these groups. Both MPO activity and cytokine IL-1β were elevated in bleomycin treated group, however, they were greatly reduced in MGIIIE treated group (Fig. 2G and H), indicating an anti-inflammatory effect of MGIIIE in bleomycin-induced lung inflammation. These data demonstrated that MGIIIE significantly attenuated lung inflammation and fibrosis in bleomycin-induced pulmonary fibrosis.

3.3. The fibrotic markers are altered by MGIIIE during bleomycin-induced pulmonary fibrosis

Hydroxyproline (HYP), α-SMA, collagen I (Col I) and MMP-9/TIMP-1 ratio are major fibrotic markers during pulmonary fibrosis (Li et al., 2015; Todd et al., 2012; Yoshimura et al., 2006). Hydroxyproline and Col I indicate collagen production in tissue (Li et al., 2015). α-SMA expression indicates a myofibroblast transformation after fibroblast activation. The ratio of protease MMP-9/TIMP-1 is essential for ECM remodeling (You et al., 2015). TGF-β/Smad2/3 signal is a major pro-fibrotic factor which is responsible for switching inflammatory phase to fibrotic phase in lung fibrosis (Bhattacharyya et al., 2013; Yang et al., 2012). To investigate whether MGIIIE has anti-fibrotic effect in bleomycin-induced pulmonary fibrosis, we

measured these markers in fibrotic lung tissue in MGIIIE-M and MGIIIE-H treated groups. As shown in Fig. 3**,** bleomycin significantly increased HYP level, α-SMA expression, Col I content and decreased MMP-9/TIMP-1 ratio, however, both MGIIIE-M and MGIIIE-H treatment reduced the magnitude of all these changes at both protein and mRNA level. In addition, 21 days after bleomycin injection, TGF-β and phosphorylation of its downstream signals Smad2/3 were markedly increased in mice. MGIIIE significantly inhibited TGF-β/Smad2/3 pathway activation as shown in Fig. 4. These data suggested that MGIIIE protected against lung fibrosis through regulating multiple fibrotic factors.

3.4. MGIIIE down-regulates TLR4/MyD88-MAPK signals during pulmonary fibrosis

It is well documented that LPS binding to TLR4 induces MyD88-dependent pathways and TLR4 is responsible for the initiation of pulmonary inflammation and fibrosis after acute and chronic lung injury, which is integrally involved in the TGF-β1 pathway in a feed-forward loop results in increased matrix production (Yang et al., 2012; Willis et al., 2005). To investigate whether MGIIIE regulates pulmonary fibrosis through TLR4 receptor, we measured TLR4 and its downstream signaling in MGIIIE-M and MGIIIE-H treated groups. Both immunohistochemistry staining and western blotting results has shown that TLR4 expression was upregulated in lung tissue after bleomycin treatment, however, both MGIIIE middle and high doses (10 and 20 mg/kg) significantly inhibited TLR4 expression as shown less brown color in lung tissue compared with model group (Fig. 5A and B). Consistently, TLR4 and MyD88 mRNA and protein level were significantly down-regulated after treatment with MGIIIE, compared with the bleomycin group (Fig. 5C-G), indicating MGIIIE

JPET Fast Forward. Published on March 9, 2017 as DOI: 10.1124/jpet.116.239137
This article has not been copyedited and formatted. The final version may differ from this version.

may regulate TLR4 expression during lung inflammation and fibrosis. In addition, we have measured the activity of mitogen-activated protein kinase (MAPK) family, JNK, ERK and p38, the down steam signals of TLR4/MyD88 activation. It is reported that JNK, ERK and p38 play critical roles in the development of lung fibrosis (Yoshida et al., 2002; Vittal et al., 2013; Matsuoka et al., 2002; Madala et al., 2012; van der Velden et al., 2016). In our results, phosphorylation of JNK, ERK and p38 were significantly enhanced after bleomycin injection, however, their activation was inhibited by MGIIIE-H or MGIIIE–M, to a similar extent to Prednisone (Fig. 5H and I). These data indicated that MGIIIE suppressed both of TLR4/MyD88 expression and its downstream MPAK signals activation, which may contribute to its anti-fibrotic effects in pulmonary fibrosis.

3.5. MGIIIE suppressed ECM deposition and TLR4/MyD88 MAPK signaling pathway in activated lung fibroblast induced by TGF-β

Pulmonary fibroblasts transform into myofibroblast-like cells and are the one of key steps in initiation of pulmonary fibrosis. Myofibroblasts are major source of extracellular matrix production in the fibrotic lung (Hay et al., 1991). To further investigate the mechanism underlying MGIIIE inhibitory role on fibrosis in lung, primary lung fibroblasts were isolated from mice and subjected to TGF-β challenge to induce fibrosis *in vitro* model, which characterized as myofibroblast transformation and excessive collagen production in fibroblasts. First, our data showed that cell viability of fibroblast was not affected by MGIIIE (0.1-10 μM) (Fig. 6A). Second, our data showed that α-SMA and Col I expressions were greatly increased in TGF-β-treated fibroblasts, however, after MGIIIE incubation, a-SMA and Col I expressions were significantly reduced, almost to an extent similar to control group,

JPET Fast Forward. Published on March 9, 2017 as DOI: 10.1124/jpet.116.239137
This article has not been copyedited and formatted. The final version may differ from this version.

confirmed the anti-fibrotic role of MGIIIE *in vitro* (Fig. 6B-D). Moreover, both western blotting and inmmunoflurescence staining show that TLR4/MyD88 and its down-steam MAPK cascades upregulated by TGF-β are significantly inhibited by MGIIIE (Fig. 6B, E-I). Consistent with data obtained *in vivo*, these data confirmed that MGIIIE inhibit fibroblast activation and ECM deposition and its anti-fibrotic effect may act through regulating TLR4/MyD88 signaling.

3.6. MGIIIE inhibited collagen production mainly through TLR4/MyD88 MAPK signaling in activated fibroblast induced by LPS

LPS-induced fibrosis in lung fibroblasts is another well established *in vitro* model for pulmonary fibrosis. We investigated the anti-fibrotic role of MGIIIE in LPS model as well. Similarly, fibroblasts were incubated with LPS in presence or absence of MGIIIE and α-SMA and Col I contents were measured by western blotting. Consistently, MGIIIE exhibited an anti-fibrotic effect as shown a much lower α-SMA and Col I contents compared with control group (Fig. 7C, E and F). To test whether MGIIIE act through TLR4 pathway mainly or not, PLFs in some group were co-treated with MGIIIE and TAK-242, a specific antagonist of TLR4. Single addition of TAK-242 or combination with MGIIIE showed not cell toxicity on PLFs (Fig. 7A and B). LPS induced a robust expression of TLR4 in fibroblasts, however, TAK-242 significantly blocked LPS-induced fibroblast activation and collagen production, indicating LPS-induced fibrosis is TLR4 dependent (Fig. 7C-F). When co-treated with TAK-242 in fibroblast, MGIIIE failed to further reduce α-SMA and Col I contents compared with MGIIIE only group (Fig. 7C-F), indicating MGIIIE may inhibit fibrosis mainly through TLR4 signals. Taken together, these data demonstrate that MGIIIE also inhibited fibroblast activation and collagen production induced by LPS

and its inhibitory effect may through down-regulating TLR4/MyD88-MAPKs signaling pathways.

JPET Fast Forward. Published on March 9, 2017 as DOI: 10.1124/jpet.116.239137
This article has not been copyedited and formatted. The final version may differ from this version.

4. Discussion

The fruit of *Siraitia grosvenorii* Swingle (Cucurbitaceae) is a famous traditional Chinese herb for treatment of dry cough, sore throat, extreme thirst and constipation (Committee of National Pharmacopoeia, 2010). Previous study has showed that Mogroside V has protective effects on LPS-induced acute lung injury (Shi et al., 2014). Mogroside IIIE (MGIIIE) was one of cucurbitane-type triterpene glycosides (mogrosides) isolated from the fruits of *S. grosvenorii* (Xu et al., 2015). MGIIIE showed stronger inhibitory effects on maltase than Mogroside V (Suzuki et al., 2005), however, no studies have investigated the effect of MGIIIE in fibrosis. In this study, using both in vitro and in vivo model, we demonstrated, for the first time, that, MGIIIE significantly reduced fibrosis in bleomycin-induced pulmonary fibrosis mouse model and its anti-fibrotic effect may due to its inhibition on fibroblast activation and ECM deposition through downregulating TLR4 signal in fibroblasts.

Idiopathic pulmonary fibrosis (IPF) is a chronic, progressive, and irreversible lung injury. There are no effective therapies in clinic (Hashimoto et al., 2004). Bleomycin-induced pulmonary fibrosis in mouse is frequently-used mouse model to study the pathogenesis of pulmonary fibrosis. After bleomycin administration, the expression of inflammatory cytokines elevates quickly and returns to background levels 9 days after injection, while profibrotic gene expression peaks between 7 and 14 days and remains a high level up to 21 days, suggesting a “switch” between inflammation and fibrosis in this interval (Chaudhary et al., 2006). Therefore, 7 day was chosen as a time point for MGIIIE administration to investigate its anti-fibrotic effect. Our data has shown that MGIIIE is a potent inhibitor for pulmonary fibrosis in bleomycin model.

In IPF, the predominant cell types are the fibroblasts and myofibroblasts.

Inflammatory damage to the effected epithelium results in the secretion of growth factors, which stimulate the underlying fibroblast transforming to myofibroblasts. Myofibroblasts secrete growth factors and ECM components and contribute to increased collagen deposition and eventually leads to fibrosis (Bocchino et al., 2010). Many inflammatory cytokines and pro-fibrotic factors are involved in the fibrosis process, among which, IL-1β, MPO, TGF-β, MMP-9/TIMP, a-SMA, collagen I are the most important players. IL-1β, MPO are the pro-inflammatory factors mediating a lung inflammation after bleomycin injection. TGF-β is a major inducer for fibroblast activation to myofibroblast (Wynn, 2007). MMP-9 causes collagen degradation, while TIMPs play a pivotal role in control of MMP catalytic activity in fibrogenesis (Chen et al., 2012). The ratio of MMP-9/TIMP inversely controls ECM deposition in lung fibrogenesis (You et al., 2015). α-SMA is a marker for myofibroblasts and collagen I are hallmark for fibrosis (Li et al., 2015). In our study, MGIIIE significantly inhibited expression of TGF-β, α-SMA and collagen I and increased MMP-9/TIMP ratio, indicating MGIIIE inhibit fibrosis through regulating fibrotic factors. In addition, our data has shown MGIIIE inhibited MPO and IL-1β level induced by bleomycin indicating that MGIIIE may have anti-inflammatory effects, which may contribute to lung fibrosis attenuation. In the future, the anti-inflammatory effects of MGIIIE including inflammatory cytokine expression and neutrophil or macrophage infiltration will be evaluated at earlier time points (1-6 days after bleomycin injection) during inflammation phase.

It is well documented that LPS or TGF-β can induce fibroblast activation and collagen deposition in cultured lung fibroblasts (Bhattacharyya et al., 2013). In cell model of transdifferentiation of quiescent fibroblasts into myofibroblasts with TGF-β1 induction, primary mouse lung fibroblasts (PLFs) acquired a mesenchymal

JPET Fast Forward. Published on March 9, 2017 as DOI: 10.1124/jpet.116.239137
This article has not been copyedited and formatted. The final version may differ from this version.

phenotype and a higher α-SMA expression (Sun et al., 2015). While, LPS induces fibrosis by increasing a rapid release of pro-inflammatory cytokines, which activates fibroblasts as well (Krebs et al., 2015; Synenki et al., 2007). Using these two *in vitro* fibrosis models, our data showed that MGIIIE significantly inhibited fibroblast activation and collagen production in PLFs induced by LPS or TGF-β and confirmed anti-fibrotic effects of MGIIIE in lung fibrosis.

TLR4 has shown essential for protective immunity against infection during the pathogenesis of fibrosis (Jiang et al., 2005). MyD88 serves as a key TLR4 adaptor protein, linking the receptors to downstream kinases, deficiency of MyD88 protects mice from inflammation and fibrosis after bleomycin treatment indicating TLR4/MyD88 may be specific target for inflammatory responses (Salaun et al., 2007; Gasse et al., 2007). In addition, extensive evidence has shown that down stream signals of TLR4, JNK, ERK and p38 robustly increased in IPF patients and pharmacological inhibition of these three MAPKs significantly reduced fibrosis in mice and patients (Yoshida et al., 2002; Vittal et al., 2013; Matsuoka et al., 2002; Madala et al., 2012; van der Velden et al., 2016; Moran, 2011). Inhibited TGF-β1 and pulmonary fibrosis was observed in JNK knockout mice indicating JNK is required for fibrosis development (Alcorn et al., 2009). PD98059, a highly selective inhibitor of ERK activation ameliorated lung injury and pulmonary fibrosis (Galuppo et al., 2011), and a p38 inhibitor has been approved for IPF treatment in Europe (Moran, 2011). In bleomycin-induced pulmonary fibrosis mouse model, our data showed that MGIIIE significantly decreased expressions of TLR4/MyD88, as well as phosphorylations of MAPKs (including JNK, ERK and p38). In addition, TLR4 specific inhibitor, TAK-242 blocked LPS-induced fibroblast activation confirming the essential role of TLR4 in fibroblast activation. Consistently, MGIIIE markedly

decreased TLR4/MyD88 and collagen synthesis induced by LPS or TGF-β, suggesting that MGIIIE may inhibit fibrosis through regulating TLR4 signaling. Moreover, MGIIIE failed to induce further reduction of collagen production after TAK-242 pretreatment on fibroblasts, implicating MGIIIE may inhibit fibrosis mainly through TLR4 expression, however, more direct evidence is needed before drawing this conclusion. Currently, our lab is investigating whether TLR4 is required for anti-fibrotic effects of MGIIIE by performing rescue experiments using a lentival-TLR4 overexpressing system in PLFs.

In summary, the present study demonstrated that MGIIIE protected against bleomycin-induced pulmonary fibrosis both *in vitro* and *in vivo* and its anti-fibrotic effect may due to inhibiting fibroblast activation and collagen deposition regulated by TLR4 signals. These findings provide new insights in understanding the bioactivity of MGIIIE. MGIIIE may have therapeutic potential for the treatment of pulmonary fibrosis in clinic applications.

JPET Fast Forward. Published on March 9, 2017 as DOI: 10.1124/jpet.116.239137
This article has not been copyedited and formatted. The final version may differ from this version.

Acknowledgments

We gratefully acknowledge the Chengdu Biopurify Phytochemical Ltd. (Chengdu, China) for the generous gifts of Mogroside IIIE (MGIIIE, purity above 99%), Mogroside IVE (MGIVE, purity above 99%), Siamenoside I (SMI, purity above 99%) and Mogroside V (MGV, purity above 99%).

Authorship Contributions

L.J. Tao, H.F. Xie, Y.Q. Gong and C.F. Zhang participated in research design, L.J. Tao, Y.Q. Gong and C.F Zhang conducted experiments, L.J. Tao, J.Y. Yang and F.Y. Cao performed data analysis, L.J. Tao,M. Zhang, Y.Q. Gong and C.F Zhang wrote or contributed to the writing of the manuscript.

References

Alcorn JF, van der Velden J, Brown AL, McElhinney B, Irvin CG, Janssen-Heininger YM (2009) c-Jun N-terminal kinase 1 is required for the development of pulmonary fibrosis. *Am J Respir Cell Mol Biol* **40:** 422–432.

Bhattacharyya S, Kelley K, Melichian DS, Tamaki Z, Fang F, Su YY, Feng G, Pope RM, Scott Budinger GR, Mutlu GM, Lafyatis R, Radstake T, Feghali-Bostwick C, Varga J (2013) Toll-Like receptor 4 signaling augments transforming growth factor-β responses: a novel mechanism for maintaining and amplifying fibrosis in scleroderma. *Am J Pathol* **182:** 192–205.

Bocchino M, Agnese S, Fagone E, Svegliati S, Grieco D, Vancheri C, Gabrielli A, Sanduzzi A, Awedimento EV (2010) Reactive oxygen species are required for maintenance and differentiation of primary lung fibroblasts in idiopathic pulmonary fibrosis. *PLoS One* **5:** e14003.

Bruce MC, Honaker CE (1998) Transcriptional regulation of tropoelastin expression in rat lung fibroblasts: changes with age and hyperoxia. *Am J Physiol* **274:** L940–L950.

Chaudhary NI, Schnapp A, Park JE (2006) Pharmacologic differentiation of inflammation and fibrosis in the rat bleomycin model. *Am J Respir Crit Care Med* **173:** 769–776.

Chen ML, Cheung FW, Chan MH, Hui PK, Ip SP, Ling YH, Che CT, Liu WK (2012) Protective roles of Cordyceps on lung fibrosis in cellular and rat models. *J Ethnopharmacol* **143:** 448–454.

Chen XB, Zhuang JJ, Liu JH, Lei M, Ma L, Chen J, Shen X, Hu LH (2011) Potential AMPK activators of cucurbitane triterpenoids from Siraitia grosvenorii Swingle. *Bioorg Med Chem* **19:** 5776–5781.

Committee of National Pharmacopoeia (2010) Pharmacopoeia of P.R. China. *Chemical Industry Press Beijing* 197.

Derynck R, Zhang YE (2003) Smad-dependent and Smad-independent pathways in TGF-β family signaling. *Nature* **425:** 577–584.

Di R, Huang MT, Ho CT (2011) Anti-inflammatory activities of mogrosides from Momordica grosvenori in murine macrophages and a murine ear edema model. *J Agric Food Chem* **59:** 7474–7481.

Fan HY, Qi D, Yang MY, Fang H, Liu K, Zhao F (2013) In vitro and in vivo anti-inflammatory effects of 4-methoxy-5-hydroxycanthin-6-one, a natural alkaloid from Picrasma quassioides. *Phytomedicine* **20:** 319–323.

Galuppo M, Esposito E, Mazzon E, Di Paola R, Paterniti I, Impellizzeri D, Cuzzocrea S (2011) MEK inhibition suppresses the development of lung fibrosis in the bleomycin model. *Naunyn Schmiedebergs Arch Pharmacol* **384:** 21–37.

Gasse P, Mary C, Guenon I, Noulin N, Charron S, Schnyder-Candrian S, Schnyder B, Arika S, Quesniaux VF, Lagente V, Ryffel B, Couillin I (2007) IL-1R1/Myd88 signaling and the inflammasome are essential in pulmonary inflammation and fibrosis in mice. *J Clin Invest* **117:** 3786–3799.

Gürbüzel M, Sayar I, Cankaya M, Gürbüzel A, Demirtas L, Bakirci EM, Capoglu I (2016) The preventive role of levosimendan against bleomycin-induced pulmonary fibrosis in rats. *Pharmacol Rep* **68:** 378–382.

Hashimoto N, Jin H, Liu T, Chensue SW, Phan SH (2004) Bone marrow-derived progenitor cells in pulmonary fibrosis. *J Clin Invest* **113:** 243–252.

Hay J, Shahzeidi S, Laurent G (1991) Mechanisms of bleomycin-induced lung damage. *Arch Toxicol* **65:** 81–94.

He ZY, Gao Y, Deng YX, Li W, Chen YM, Xing SP, Zhao XY, Ding J, Wang XR

(2012) Lipopolysaccharide induces lung fibroblast proliferation through Toll-like receptor 4 signaling and the phosphoinositide3-kinase-Akt pathway. *PLoS One* **7:** e35926.

He ZY, Zhu YS, Jiang H (2009) Inhibiting toll-like receptor 4 signaling ameliorates pulmonary fibrosis during acute lung injury induced by lipopolysaccharide: an experimental study. *Respir Res* **10:** 126.

Huebener P, Schwabe RF (2013) Regulation of wound healing and organ fibrosis by toll-like receptors. *Biochim Biophys Acta* **1832:** 1005–1017.

Jiang DH, Liang JR, Fan J, Yu S, Chen SP, Luo Y, Prestwich G, Mascarenhas MM, Garg HG, Quinn DA, Homer RJ, Goldstein DR, Bucala R, Lee PJ, Medzhitov R, Noble PW (2005) Regulation of lung injury and repair by Toll-like receptors and hyaluronan. *Nat Med* **11:** 1173–1179.

Jin JS, Lee JH (2012) Phytochemical and pharmacological aspects of Siraitia grosvenorii, luo han kuo. *Orient Pharm Exp Med* **12:** 233–239.

Krebs J, Kolz A, Tsagogiorgas C, Pelosi P, Rocco PR, Luecke T (2015) Effects of lipopolysaccharide-induced inflammation on initial lung fibrosis during open-lung mechanical ventilation in rats. *Respir Physiol Neurobiol* **212–214:** 25–32.

Li LC, Li DL, Xu L, Zhao P, Deng ZY, Mo XT, Li P, Qi LW, Li J, Gao J (2015) Total extract of Yupingfeng attenuates bleomycin-induced pulmonary fibrosis in rats. *Phytomedicine* **22:** 111–119.

Madala SK, Schmidt S, Davidson C, Ikegami M, Wert S, Hardie WD (2012) MEK-ERK pathway modulation ameliorates pulmonary fibrosis associated with epidermal growth factor receptor activation. *Am J Respir Cell Mol Biol* **46:** 380–388.

Matsuoka H, Arai T, Mori M, Goya S, Kida H, Morishita H, Fujiwara H, Tachibana I, Osaki T, Hayashi S (2002) A p38 MAPK inhibitor, FR-167653, ameliorates murine bleomycin-induced pulmonary fibrosis. *Am J Physiol Lung Cell Mol Physiol* **283:** L103–L112.

Moran N (2011) p38 kinase inhibitor approved for idiopathic pulmonary fibrosis. *Nat Biotechnol* **29:** 301.

Poltorak A, He X, Smirnova I, Liu MY, Van Huffel C, Du X, Birdwell D, Alejos E, Silva M, Galanos C, Freudenberg M, Ricciardi-Castagnoli P, Layton B, Beutler B (1998) Defective LPS signaling in C3H/HeJ and C57BL/10ScCr mice: mutations in Tlr4 gene. *Science* **282:** 2085–2088.

Rhieu BH, Epperly MW, Cao S, Goff J, Shields D, Franicola D, Wang H, Greenberger JS (2014) Improved longevity of hematopoiesis in long-term bone marrow cultures and reduced irradiation-induced pulmonary fibrosis in Toll-like receptor-4 deletion recombinant-negative mice. *In Vivo* **28:** 441–448.

Salaun B, Romero P, Lebecque S (2007) Toll-like receptors' two-edged sword: when immunity meets apoptosis. *Eur J Immunol* **37:** 3311–3318.

Shi DF, Zheng MZ, Wang YM, Liu CM, Chen S (2014) Protective effects and mechanisms of mogroside V on LPS-induced acute lung injury in mice. *Pharm Biol* **52:** 729–734.

Song KJ, Liao ZX, Liu YP, Chen XY, Huang CH (2014) Effect of activation and apoptosis of mogroside on hepatic stellate cell. *Chinese Traditional Patent Medicine* **36:** 481–484.

Sun BS, Chen YP, Wang YB, Tang SW, Pan FY, Li Z, Sung CK (2012) Anti-obesity effects of mogrosides extracted from the fruits of Siraitia grosvenorii (Cucurbitaceae). *Afr J Pharm Pharmacol* **6:** 1492–1501.

Sun X, Chen E, Dong R, Chen WG, Hu Y (2015) Nuclear factor (NF)-κB p65 regulates differentiation of human and mouse lung fibroblasts mediated by TGF-β. *Life Sic* **122:** 8–14.

Suzuki YA, Murata Y, Inui H, Sugiura M, Nakano Y (2005) Triterpene glycosides of Siraitia grosvenori inhibit rat intestinal maltase and suppress the rise in blood glucose level after a single oral administration of maltose in rats. *J Agric Food Chem* **53:** 2941–2946.

Synenki L, Chandel NS, Budinger GR, Donnelly HK, Topin J, Eisenbart J, Jovanovic B, Jain M (2007) Bronchoalveolar lavage fluid from patients with acute lung injury/acute respiratory distress syndrome induces myofibroblast differentiation. *Crit Care Med* **35:** 842–848.

Szapiel SV, Elson NA, Fulmer JD, Hunninghake GW, Crystal RG (1979) Bleomycin-induced interstitial pulmonary disease in the nude, athymic mouse. *Am Rev Respir Dis* **120:** 893–899.

Todd NW, Luzina IG, Atamas SP (2012) Molecular and cellular mechanisms of pulmonary fibrosis. *Fibrogenesis Tissue Repair* **5:** 11.

van der Velden JL, Ye Y, Nolin JD, Hoffman SM, Chapman DG, Lahue KG, Abdalla S, Chen P, Liu Y, Bennett B, Khalil N, Sutherland D, Smith W, Horan G, Assaf M, Horowitz Z, Chopra R, Stevens RM, Palmisano M, Janssen-Heininger YM, Schafer PH (2016) JNK inhibition reduces lung remodeling and pulmonary fibrotic systemic markers. *Clin Transl Med* **5:** 36.

Vittal R, Fisher A, Gu H, Mickler EA, Panitch A, Lander C, Cummings OW, Sandusky GE, Wilkes DS (2013) Peptide-mediated inhibition of mitogen-activated protein kinase-activated protein kinase-2 ameliorates bleomycin-induced pulmonary fibrosis. *Am J Respir Cell Mol Biol* **49:** 47–57.

Willis BC, Liebler JM, Luby-Phelps K, Nicholson AG, Crandall ED, du Bois RM, Borok Z (2005) Induction of epithelial–mesenchymal transition in alveolar epithelial cells by transforming growth factor-beta1: potential role in idiopathic pulmonary fibrosis. *Am J Pathol* **166:** 1321–1332.

Wynn TA (2007) Common and unique mechanisms regulate fibrosis in various fibroproliferative diseases. *J Clin Invest* **117:** 524–529.

Xiao G, Chen Z, Li WN, Wang Q, Liao CX (2012) Protective effect of mogroside on carbon tetrachloride-induced hepatic fibrosis rats. *Shandong Medicine* **52:** 19–24.

Xiao G, Wang Q (2013) Experiment study on the hepatoprotective effect of mogrosides. *Chinese Journal of Experimental Traditional Medical Formulae* **19:** 196–200.

Xu F, Li DP, Huang ZC, Lu FL, Wang L, Huang YL, Wang RF, Liu GX, Shang MY, Cai SQ (2015) Exploring in vitro, in vivo metabolism of mogroside V and distribution of its metabolites in rats by HPLC-ESI- IT-TOF-MS^n. *J Pharm Biomed Anal* **115:** 418–430.

Yang HZ, Wang JP, Mi S, Liu HZ, Cui B, Yan HM, Yan J, Li Z, Liu H, Hua F, Lu W, Hu ZW (2012) TLR4 activity is required in the resolution of pulmonary inflammation and fibrosis after acute and chronic lung injury. *Am J Pathol* **180:** 275–292.

Yoshida K, Kuwano K, Hagimoto N, Watanabe K, Matsuba T, Fujita M, Inoshima I, Hara N (2002) MAP kinase activation and apoptosis in lung tissues from patients with idiopathic pulmonary fibrosis. *J Pathol* **198:** 388–396.

Yoshimura S, Nishimura Y, Nishiuma T, Yamashita T, Kobayashi K, Yokoyama M (2006) Over expression of nitric oxide synthase by the endothelium attenuates

bleomycin-induced lung fibrosis and impairs MMP-9/TIMP-1 balance. *Respirology* **11:** 546–556.

You XY, Xue Q, Fang Y, Liu QY, Zhang CF, Zhao C, Zhang M, Xu XH (2015) Preventive effects of Ecliptae Herba extract and its component, ecliptasaponin A, on bleomycin-induced pulmonary fibrosis in mice. *J Ethnopharmacol* **175:** 172–180.

Footnotes

This work was financially supported by the National Natural Science Foundation of China (81573553, C.F. Zhang), the National New Drug Innovation Major Project of China (2011ZX09307-002-02)，the Priority Academic Program Development of Jiangsu Higher Education Institutions (PAPD) and National Found for Fostering Talents of Basic Science (NFFTBS, J1310032) in China and American Heart Association (12SDG9050018, Y. Gong) in the U.S.

Figure legends

Figure 1 – Mogrosides inhibited NO production in LPS-activated RAW264.7 cells. RAW264.7 cells were incubated with/without LPS (5 μg/ml) in the absence or presence of four mogrosides (MGV, SMI, MGIVE and MGIIIE) at different concentrations. (A) The chemical structures of four mogrosides (MGV, SMI, MGIVE and MGIIIE). (B) Cell viability. (C) Nitric oxide levels. Data are expressed as mean ± S.D. (n = 5). $^{**}p < 0.01$, $^{***}p < 0.001$.

Figure 2 – MGIIIE treatment attenuated bleomycin-induced pulmonary fibrosis in mice. Mice were given an intragastric administration of MGIIIE (1, 10 or 20 mg/kg, respectively) and prednisone (6.5 mg/kg) daily 7 days after an *i.n.* injection of bleomycin, and mice were killed at 21 day after bleomycin injection. The body weight (A), survival rate (B) and pulmonary index (F) were determined, and the representative images of H&E staining and Masson's trichrome staining(C) of lung sections in mice as well as comparison of the inflammation score (D) and fibrosis score (E) among the experimental groups were shown. Data are expressed as mean ± S.D. (n = 10). The myeloperoxidase (MPO) activity and IL-1β level were detected in the lung tissue (G & H). Data are expressed as mean ± S.D. (n = 5). $^{###}p < 0.001$ vs. control group. $^{**}p < 0.01$, $^{***}p < 0.001$ vs. model group.

Figure 3 – MGIIIE treatment decreased the HYP content, collagen content and other fibrotic markers in bleomycin-damaged lung tissues in mice. Mice were given an intragastric administration of MGIIIE (10 and 20 mg/kg, respectively) and prednisone (6.5 mg/kg) daily 7 days after an *i.n.* injection of bleomycin, and mice were killed at 21 day after bleomycin injection. (A) The HYP content in the lung tissues were

detected. The mRNA expressions of α-SMA (B) and Col I (C) in the lung tissues were detected by real time-PCR analysis. (D-I) The protein expressions of α-SMA, Col I, MMP-9, TIMP-1 and the ratio of MMP-9/TIMP-1 in the lung tissues were detected by western blot analysis. Data are expressed as mean ± S.D. (n = 3-5). $^{###}p < 0.001$ vs. control group. $^{*}p < 0.05$, $^{**}p < 0.01$, $^{***}p < 0.001$ vs. model group.

Figure 4 – MGIIIE treatment inhibited TGF-β/Smad pathway in bleomycin-induced pulmonary fibrosis. Mice were given an intragastric administration of MGIIIE (10 and 20 mg/kg, respectively) and prednisone (6.5 mg/kg) daily 7 days after an *i.n.* injection of bleomycin, and mice were killed at 21 day after bleomycin injection. (A-C) The protein expression of TGF-β1 and its relative mRNA expression were detected by western blot and real time-PCR analyses. (B-D) Effects on the expression of Smad2/3 and its phosphorylation p-Smad2/3 were detected by western blot analysis. Data are expressed as mean ± S.D. (n = 3). $^{###}p < 0.001$ vs. control group. $^{**}p < 0.01$, $^{***}p < 0.001$ vs. model group.

Figure 5 – MGIIIE down-regulated TLR4/MyD88-MAPK signals in bleomycin-induced pulmonary fibrosis in mice. Mice were given an intragastric administration of MGIIIE (10 and 20 mg/kg, respectively) and prednisone (6.5 mg/kg) daily 7 days after an *i.n.* injection of bleomycin, and mice were killed at 21 day after bleomycin injection. Representative images of immunohistochemical analysis of TLR4 expression (A-B) in the lung section (brown). The relative mRNA levels (C-D) and protein expressions (E-G) of TLR4 and MyD88 were investigated by real time-PCR and western blot analyses. (H-I) Phosphorlations of JNK, ERK and p38 in the lung tissues. Data are expressed as mean ± S.D. (n = 3). $^{###}p < 0.001$ vs. control

group. $^{*}p < 0.05$, $^{**}p < 0.01$, $^{***}p < 0.001$ vs. model group.

Figure 6 – MGIIIE reduces ECM deposition and TLR4/MyD88-MAPK signaling pathways in PLFs induced by TGF-β1. PLFs were treated with/without TGF-β1 (10 ng/ml) in the absence or presence of MGIIIE (10 μM) for 48 h. (A) Cytotoxicity of MGIIIE on PLFs was detected by MTT assay. (B-H) Protein expression of α-SMA, Col I, TLR4, MyD88 and MAPK in PLFs; (I) Representative image of protein expression of TLR4 and α-SMA by immunofluorescence staining. Data are expressed as mean ± S.D. (n = 3-5). $^{*}p < 0.05$, $^{**}p < 0.01$, $^{***}p < 0.001$.

Figure 7 – MGIIIE inhibited fibrosis induced by LPS mainly through regulating TLR4 expression. The mouse lung fibroblasts were pretreated with/without TAK-242 (10 nM) for 1.5 h and subsequently in the absence or presence of MGIIIE (10 μM) and LPS (5 μg/ml) for 48 h. (A-B) Effects of TAK-242 and MGIIIE on mouse lung fibroblasts proliferation were measured by the MTT assays. (C-F) Expressions of TLR4, α-SMA and Col I in mouse lung fibroblasts by western blot analysis. Data are expressed as mean ± S.D. (n = 3-5). $^{*}p < 0.05$, $^{**}p < 0.01$, $^{***}p < 0.001$. NS, non-significant.

JPET Fast Forward. Published on March 9, 2017 as DOI: 10.1124/jpet.116.239137
This article has not been copyedited and formatted. The final version may differ from this version.

Table 1

Sequences of primers used for real time quantitative PCR.

Gene	Forward primer (5′-3′)	Reverse primer(5′-3′)	Product size (bp)
M-α-SMA	CCA CGA AAC CAC CTA TAA CAG C	GGA AGG TAG ACA GCG AAG CC	236
M-Collagen I	CTG ACT GGA AGA GCG GAG AG	CGG CTG AGT AGG GAA CAC AC	116
M-TGF-β_1	AGA GCC CTG GAT ACC AAC TAT TG	TGC GAC CCA CGT AGT AGA CG	286
M-TLR4	ACA CTT TAT TCA GAG CCG TTG GT	CAG GTC CAA GTT GCC GTT TC	297
M-MyD88	CAT GGT GGT GGT TGT TTC TGA C	GAC TTG GTG CAA GGG TTG GTA T	195
M-actin	CTG AGA GGG AAA TCG TGC GT	CCA CAG GAT TCC ATA CCC AAG A	208

JPET Fast Forward. Published on March 9, 2017 as DOI: 10.1124/jpet.116.239137
This article has not been copyedited and formatted. The final version may differ from this version.

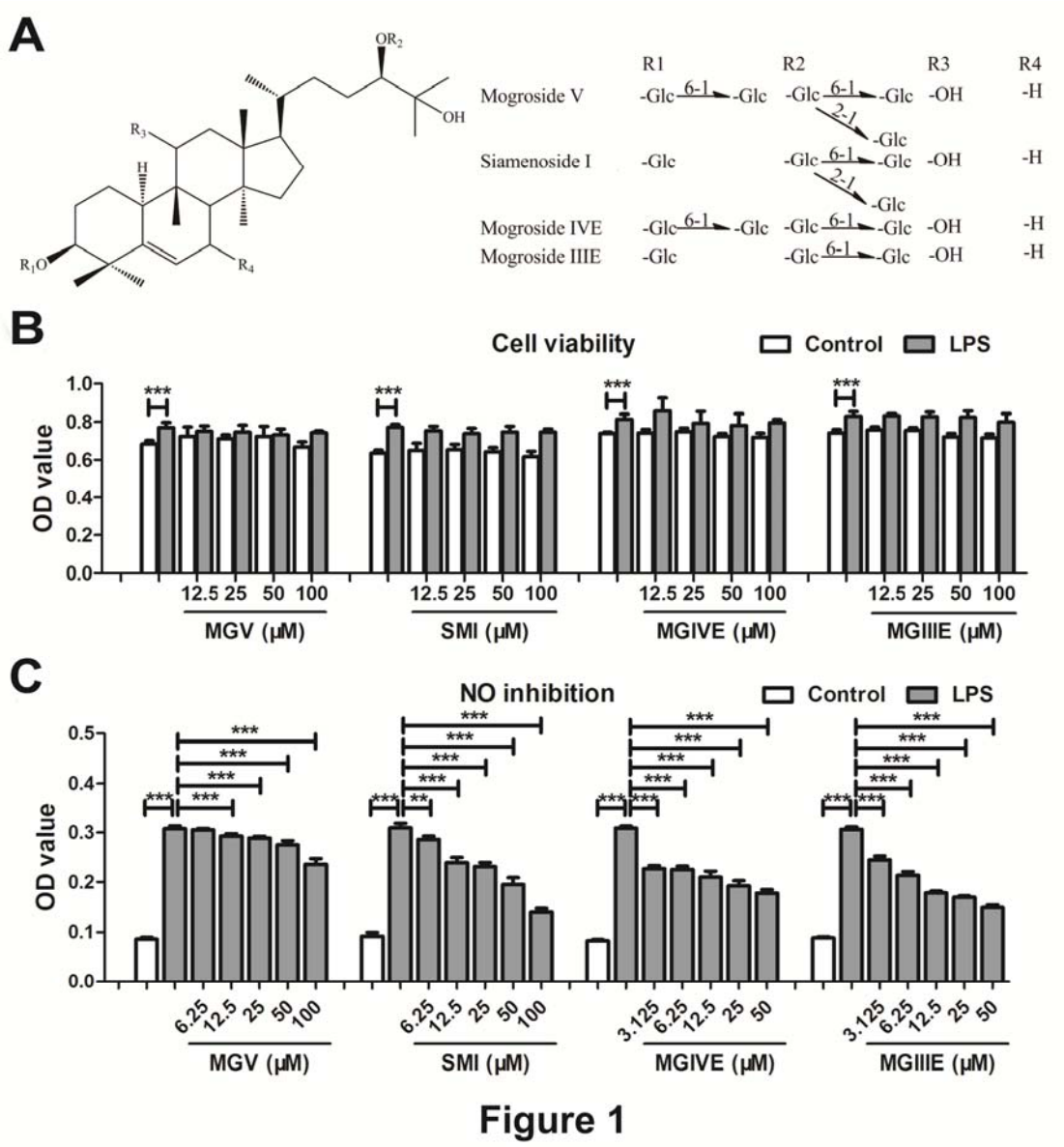

Figure 1

JPET Fast Forward. Published on March 9, 2017 as DOI: 10.1124/jpet.116.239137
This article has not been copyedited and formatted. The final version may differ from this version.

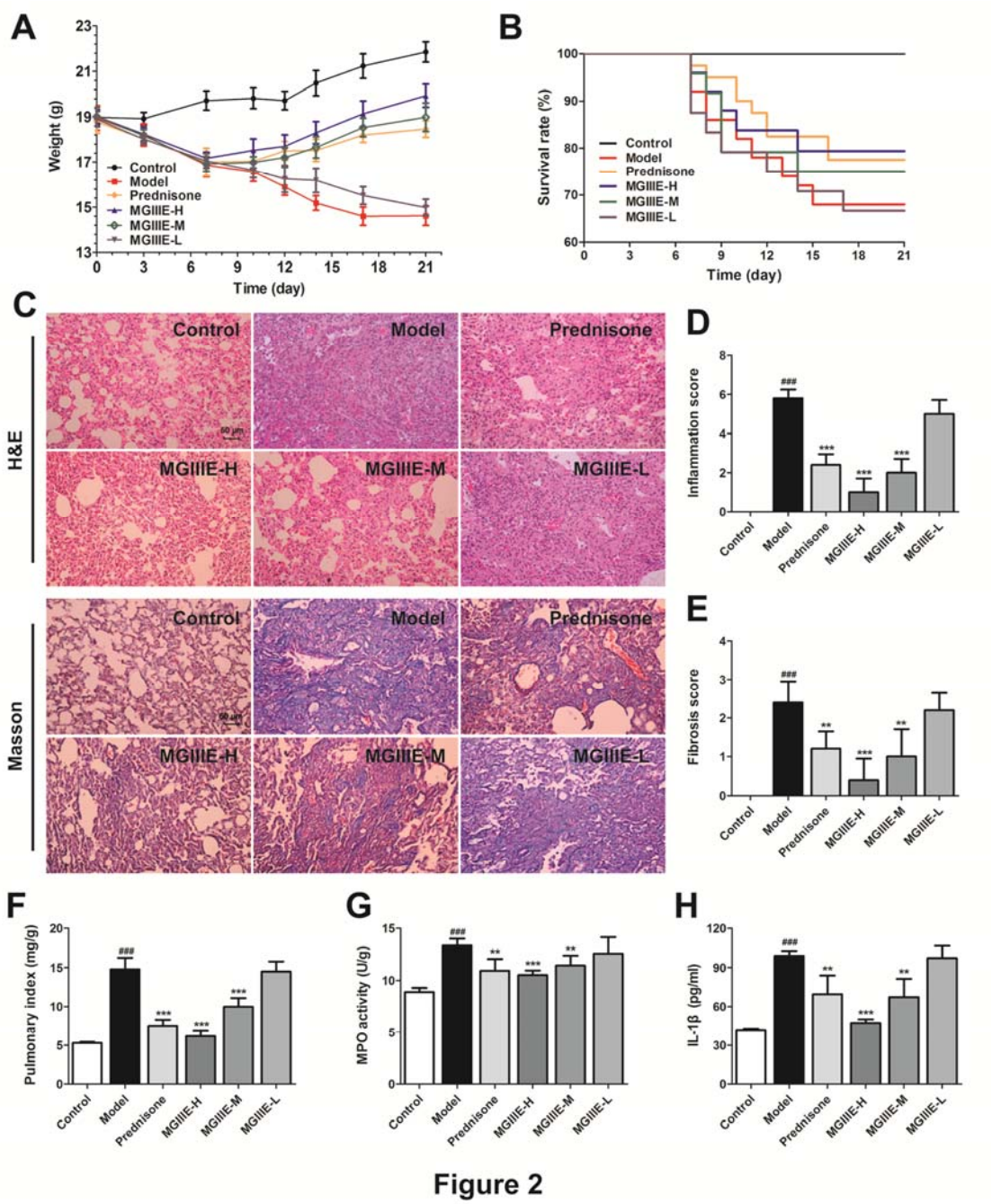

Figure 2

JPET Fast Forward. Published on March 9, 2017 as DOI: 10.1124/jpet.116.239137
This article has not been copyedited and formatted. The final version may differ from this version.

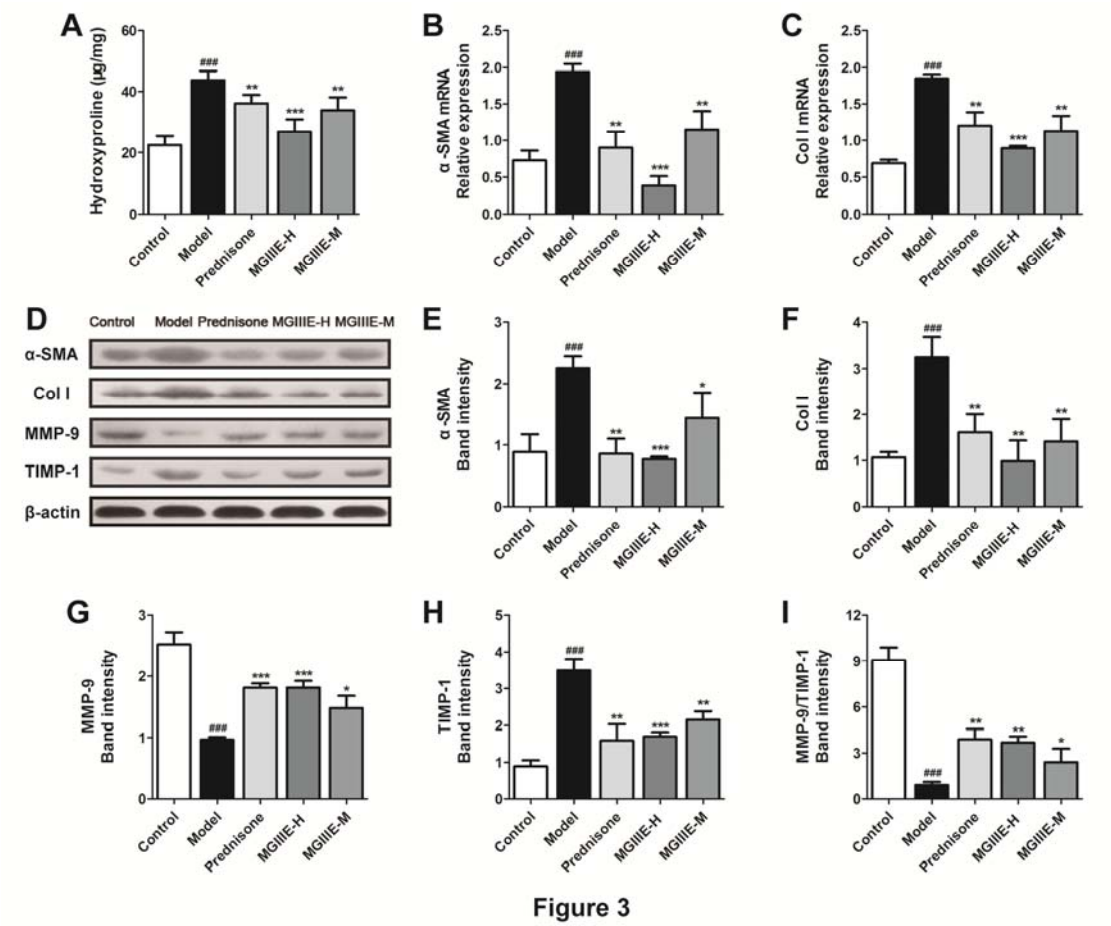

Figure 3

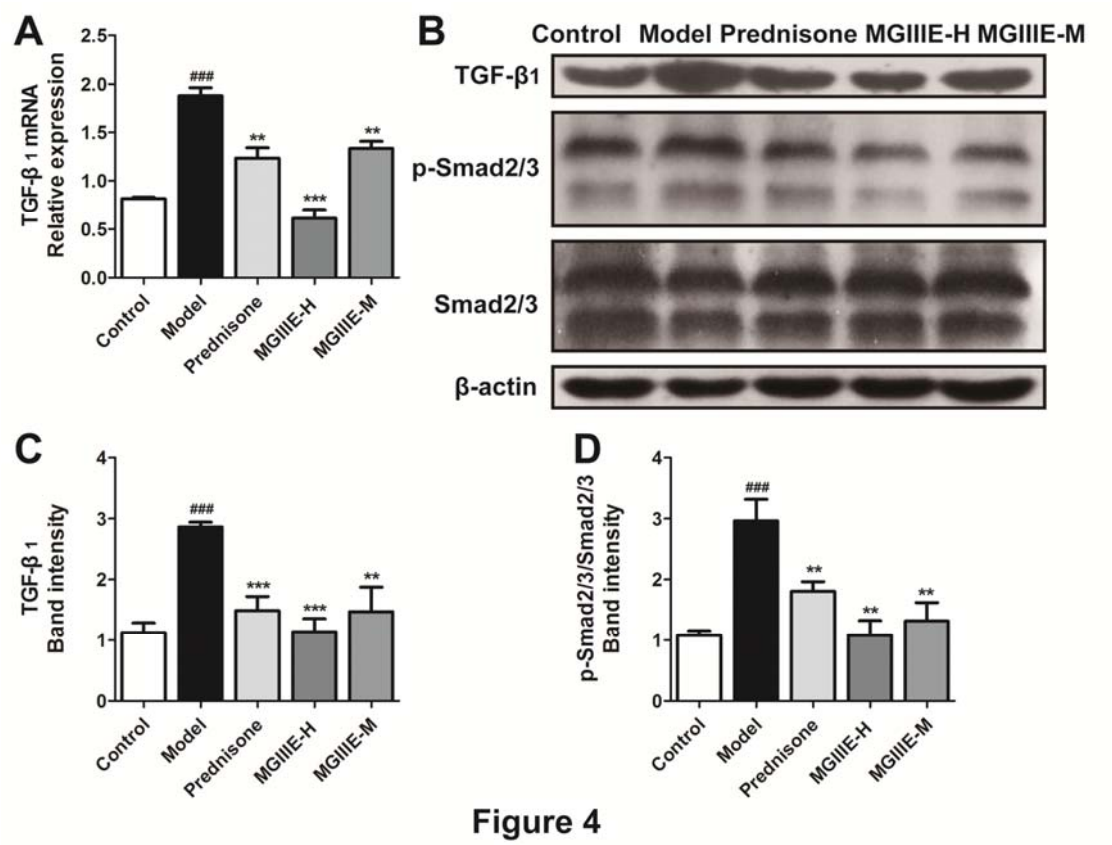

Figure 4

JPET Fast Forward. Published on March 9, 2017 as DOI: 10.1124/jpet.116.239137
This article has not been copyedited and formatted. The final version may differ from this version.

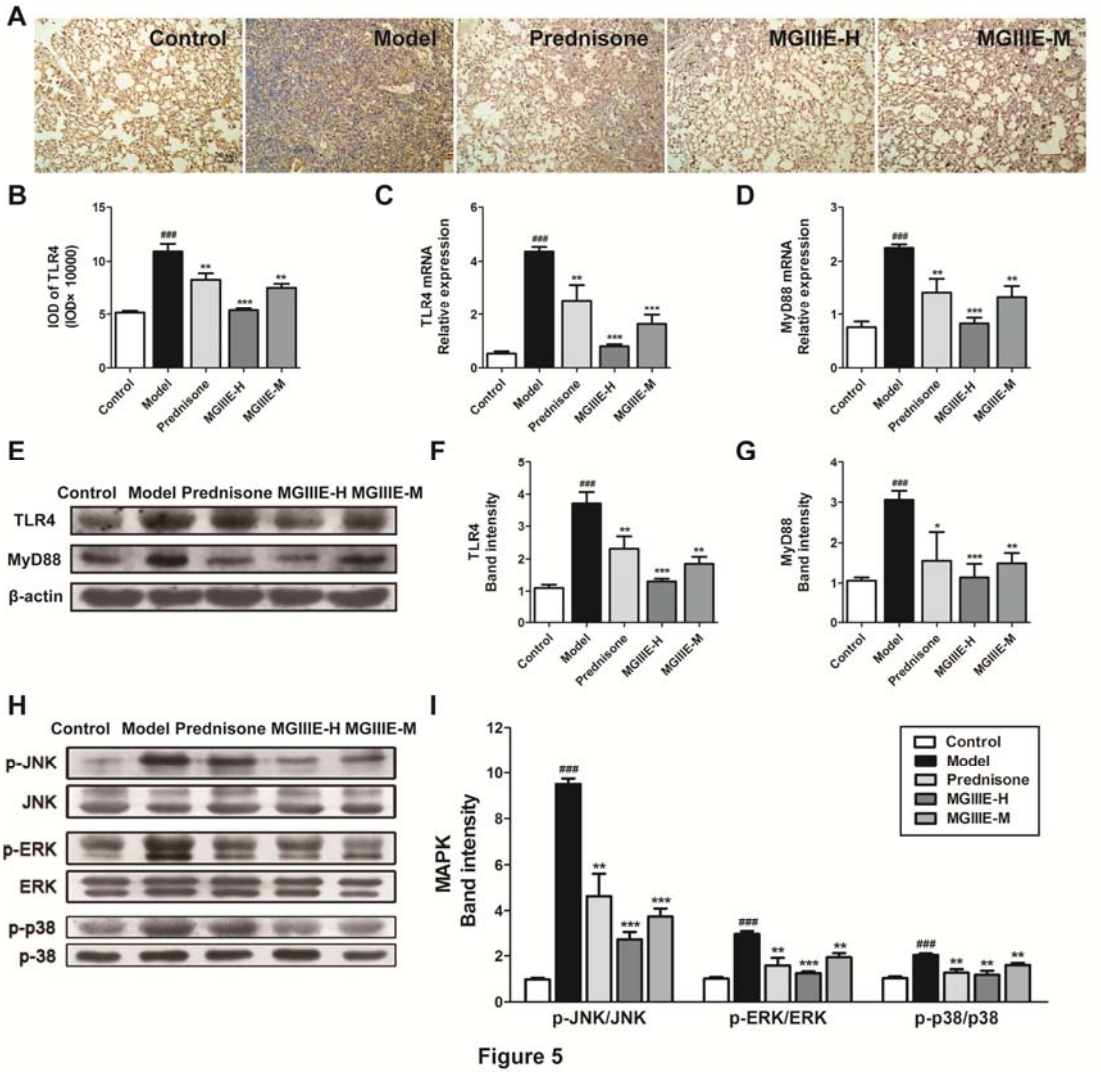

Figure 5

JPET Fast Forward. Published on March 9, 2017 as DOI: 10.1124/jpet.116.239137
This article has not been copyedited and formatted. The final version may differ from this version.

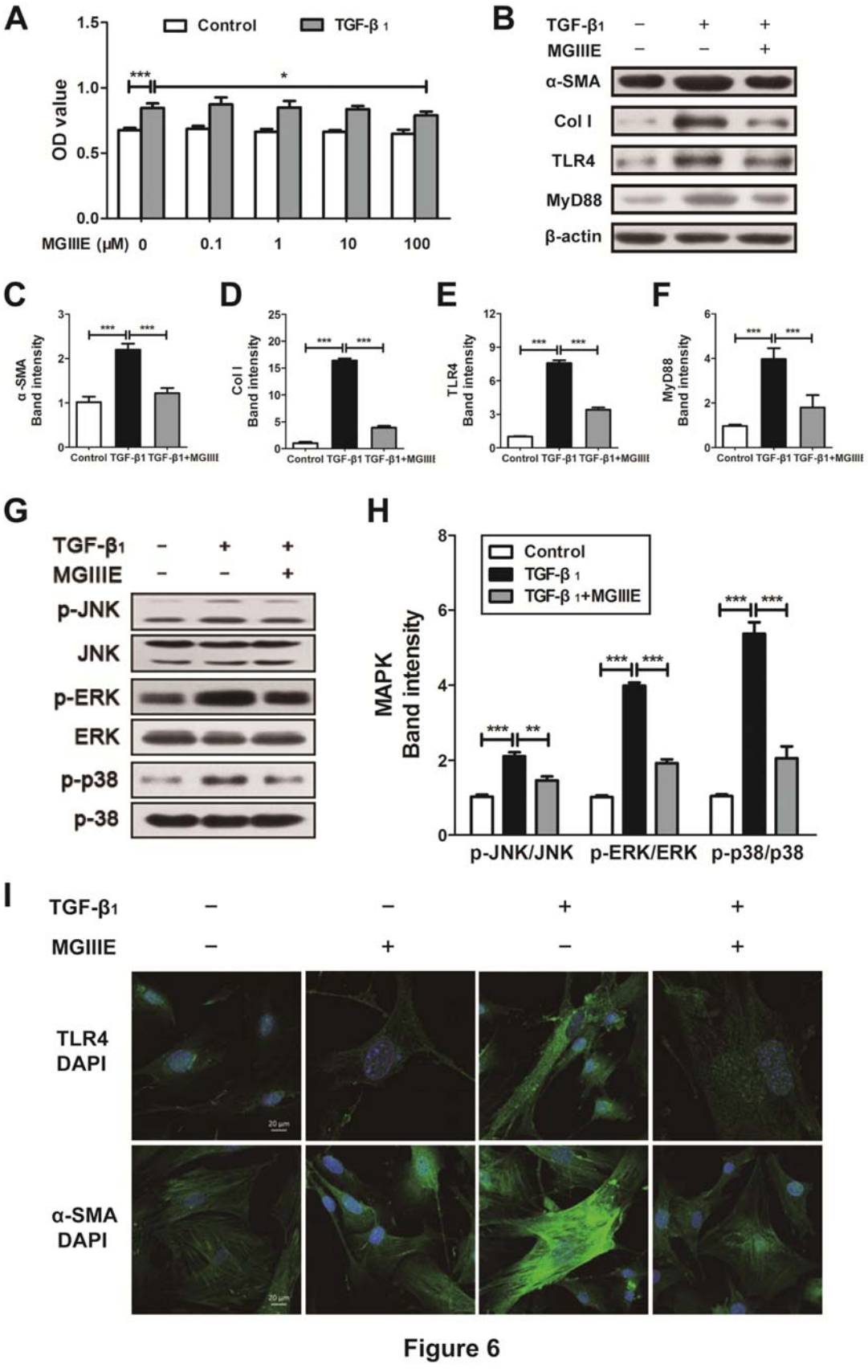

Figure 6

JPET Fast Forward. Published on March 9, 2017 as DOI: 10.1124/jpet.116.239137
This article has not been copyedited and formatted. The final version may differ from this version.

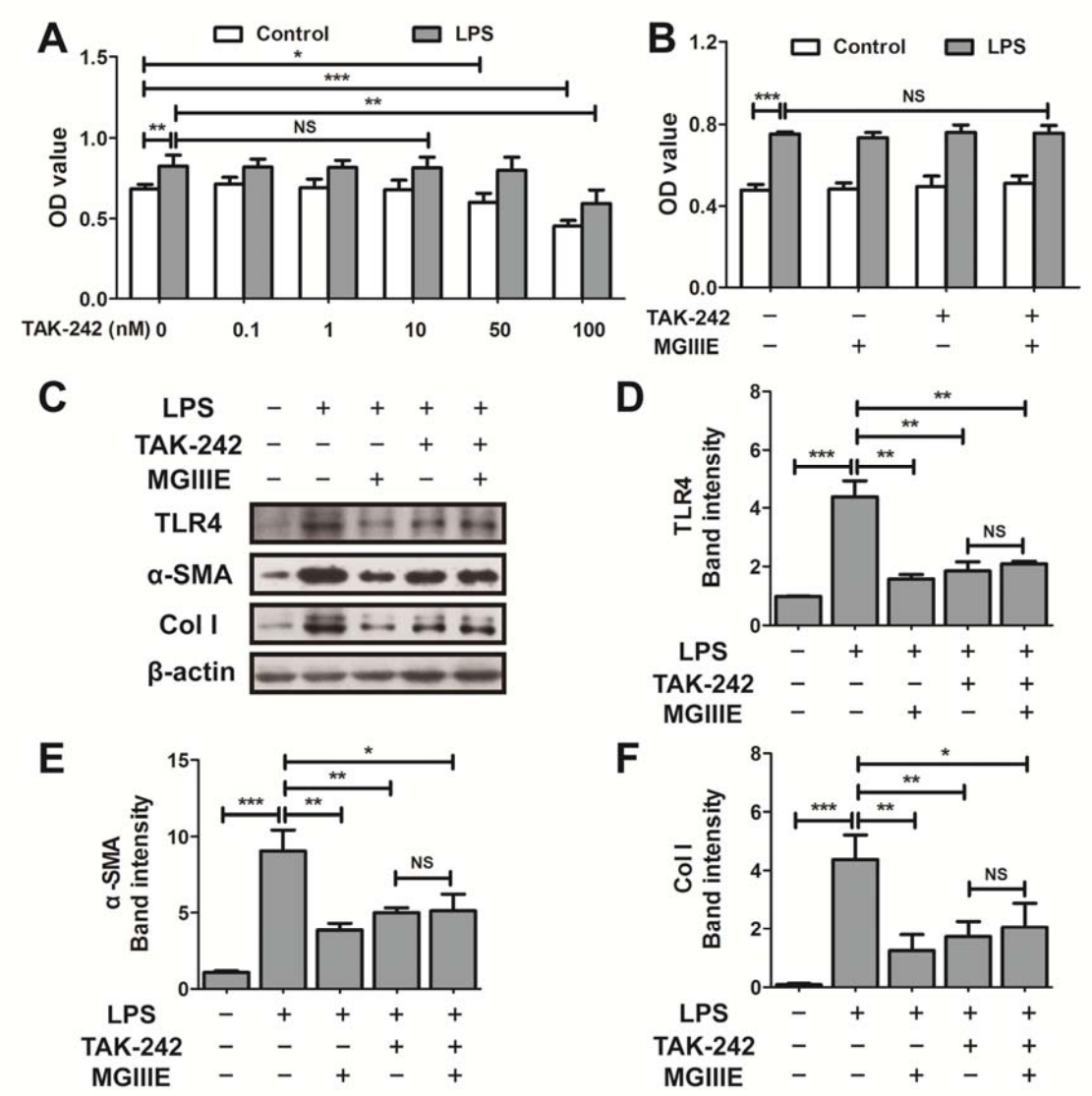

Figure 7